Preprints of the 19th World Congress
The International Federation of Automatic Control
Cape Town, South Africa. August 24-29, 2014

Optimal Race Car Motion Cueing

I. Salisbury * and D. J. N. Limebeer *

* *University of Oxford, Department of Engineering Science, Parks Road, Oxford, UK, OX1 3BN (e-mail: ingrid.salisbury@eng.ox.ac.uk, david.limebeer@eng.ox.ac.uk).*

Abstract: This paper explores the application of numerical optimal control (NOC) to the synthesis of motion cueing algorithms for race-car simulators. These techniques are used to design washout filters that address the limitations of the commonly-employed linear quadratic Guassian (LQG) regulator and classical frequency shaping strategies. The primary disadvantage of the LQG and classical tuning methods is that they do not recognise explicitly the hardware limitations of the platform and thus have to rely on an iterative process to address workspace limitations. In two new algorithms a kinematic model of the platform is used to constrain explicitly the platform's motion within the available workspace. The first algorithm is directed to the optimisation of the parameters of a linear washout filter, while in the second approach the platform motion is governed by an open-loop optimal control. The results of the two new algorithms are tested on race-car minimum lap-time simulations, and then compared with a linear-optimal-control based solution. The race-car scenario presents different challenges from the passenger car and aircraft contexts; these differences are discussed.

Keywords: Automotive Control; Motion Cueing Algorithms; Optimal Control; Parameter Optimisation.

1. INTRODUCTION

Car simulators are used in a variety of applications ranging from behavioural research to driver training and vehicle development. Regardless of the specific purpose they all aim to create a realistic environment in which the driver will behave as he/she would in a real car. In order to operate the vehicle, the driver needs a set of controls, and sensory stimuli from the vehicle and its setting (such as the vehicle's speed, its acceleration and its position on the road). This is communicated to the simulator driver through visual, auditory and motion-based cues.

The graphics are of primary importance, not only providing images of the location and driving conditions, but also for conveying the vehicular speed. Auditory cues and haptic feedback through the steering wheel and pedals also supply the driver with information about the vehicle - the engine speed and tyre slip. Acceleration and orientation is detected in humans by the vestibular system in the inner ear Dichgans and Brandt [1978]. A simulator that provides motion cues is able to stimulate this organ thereby providing a better sense of the motion of the vehicle.

Figure 1 shows the integration of various subsystems into a complete simulator and illustrates how the driver generates control commands in response to sensory cues. These inputs are fed into a vehicle model that generates a vehicle state that contains physical information about the car including its acceleration, velocity and position. This data is then used to update the visual, auditory and motion cues.

The fidelity of the simulator driving experience is always limited by the quality of the cues. Advanced 3D image

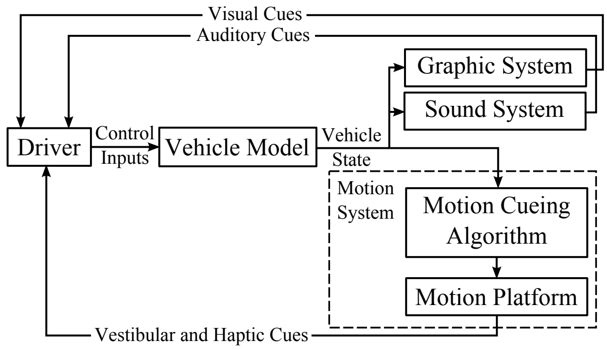

Fig. 1. Vehicle simulator components.

projection with fast refresh rates and low latency together with high-quality computer generated images (CGI) produce excellent visual cues. In the case of the motion cues the platform workspace and bandwidth restrict the quality of the cues rather than technology; to reproduce the vehicle motion exactly, the simulator would need to move in a workspace as large as the track itself. Since this is practically infeasible, different strategies have been developed to generate motion cues. While not perfect, they improve the driver's feeling of realism and thus his/her ability to drive normally. These strategies are referred to as motion cueing algorithms (MCA) and they use the vehicle's translational accelerations and its rotational velocities to move the platform appropriately without exceeding its physical limits. Most MCA development has been in the context of passenger cars and flight simulators Reid and Nahon [1985], Telban and Cardullo [2005]. In contrast, the research presented here focuses on the race car setting. This scenario differs from the passenger cars because the

Copyright © 2014 IFAC

dynamics are fast and the drivers experience much larger accelerations, particularly during cornering and braking. As a result, the race car scenario represents a more demanding MCA design challenge, not only when trying to reproduce the increased accelerations, but also with regards to the suppression of miscues that occur when the platform approaches its physical limits.

The most widely used motion cueing strategies are based on classical frequency-shaping Colombet et al. [2008], Larsen [2011] and linear-optimal-control centred algorithms Sivan et al. [1982], Reid and Nahon [1985], Telban and Cardullo [2005]. These algorithms involve the design of high-pass filters that are manually tuned so that the low-frequency demands, that would otherwise produce large displacements, are removed in order to ensure that the platform operates within its workspace limits.

The research presented in this paper makes use of general nonlinear numerical optimal control to produce motion cues. These optimal-control-based techniques are used to generate either platform accelerations directly, or to design linear filters that explicitly recognise platform workspace constraints. In both cases the problem and problem formulation are nonlinear and track specific, but the approach taken addresses the primary limitation of existing methods that only respect platform workspace limits iteratively and indirectly. This removes the repetitive tuning processes characteristic of the classical and LQG strategies.

Both the linear-optimal-control and numerical optimal control based algorithms are implemented for the yaw, lateral and longitudinal freedoms. As was previously discussed, the input to the MCA is a combination of the vehicle's translational acceleration and its angular velocity. This is usually produced by a vehicle model in response to the driver control inputs. In this study vehicle telemetry data is generated by a minimum-lap-time optimal control simulation; these details are described in Perantoni and Limebeer [2014].

The motion platform is described briefly in Sections 2. The linear optimal control approach to washout filter synthesis and the numerical optimal control algorithms that will be employed are described in Sections 3 and 4. The results and conclusions are given in Sections 5 and 6.

2. MOTION PLATFORM MODEL

The motion platform used in this study is a conventional Stewart Platform. The cab, which consists of the race car cock-pit, screens and projectors, is mounted on six actuated legs, which are connected to the platform with spherical joints and to the ground-mounted base plate with pin joints. By controlling the six actuated leg lengths the cab can be moved with 6 degrees-of-freedom (DOF).

2.1 Hexapod Kinematics

Since the boundaries of the hexapod work space are a direct consequence of the actuator stroke limits (maximum and minimum leg legnths) it is necessary to determine the hexapod leg lengths for a given platform position. These mechanics calculations are referred to as the inverse kinematics and are used in the design of motion cueing algorithms to ensure the limits of the platform are observed.

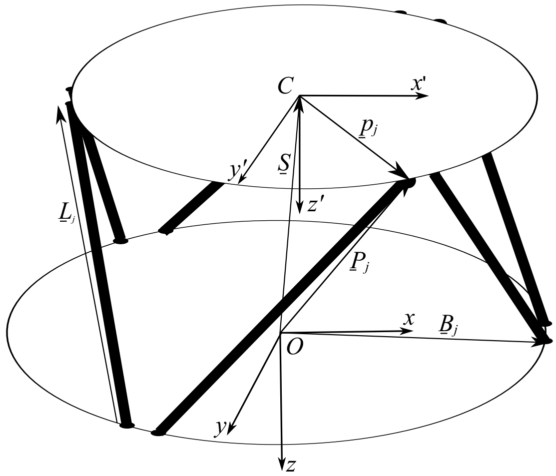

Fig. 2. Hexapod motion platform. The leg lengths are given by $\underline{L}_j$, the base attachment points by $\underline{B}_j$, and the platform attachment points by $\underline{P}_j$. The origin of the platform-fixed coordinate system is given by the vector $\underline{S}$.

The development of the kinematics equations is a standard procedure and can be found in Helinski [1990].

Referring to Figure 2, an inertial reference frame xyz with origin O is defined at the geometric centre of the hexapod base. A second body-fixed frame $x'y'z'$ is similarly defined with its origin C on the platform at the centre of the platform-leg connection joint system. The translation of the platform from the origin of the inertial reference frame is described by the vector $\underline{S}$, and the matrix R describes the platform in terms of 3 Euler angles. There are a number of choices for the Euler angles, and each configuration has distinct singularities. For consistency with the vehicle modelling, the Euler angles are chosen as 3-2-1 angles. This corresponds to a rotation first about z (yaw angle (ϕ)), then about y (roll angle (θ)) and finally about x (pitch angle (ψ)). The singularity occurs for a roll angle of $\pm\frac{\pi}{2}$, which does not occur in this application. The rotation matrix is given (where $cos(\theta)$ is abbreviated as c_θ and $sin(\theta)$ as s_θ):

$$R = R_z(\psi)R_y(\theta)R_x(\phi) \tag{1}$$

$$R = \begin{bmatrix} c_\theta c_\psi & s_\phi s_\theta c_\psi - c_\phi s_\psi & c_\phi s_\theta c_\psi + s_\phi s_\psi \\ c_\theta s_\psi & s_\phi s_\theta s_\psi + c_\phi c_\psi & c_\phi s_\theta s_\psi - s_\phi c_\psi \\ -s_\theta & s_\phi c_\theta & c_\phi c_\theta \end{bmatrix}. \tag{2}$$

The base joints of the hexapod legs are described by six vectors $\underline{B}_j$ in the inertial frame, and the platform joints are described by vectors $\underline{p}_j$ in the body-fixed frame. The platform joints can then be described by vectors $\underline{P}_j$ in the inertial frame, which are related to $\underline{p}_j$ by:

$$\underline{P}_j = \underline{S} + R \cdot \underline{p}_j \quad (j = 1 \ldots 6). \tag{3}$$

The platform legs can be described by vectors $\underline{L}_j$, which point from the base joints to the corresponding platform joints and can be found as the difference between the platform and base vectors. The leg lengths (L_j) are simply the magnitude of the leg vectors and $\hat{\underline{L}}_j$ are unit vectors associated with the directions of the legs.

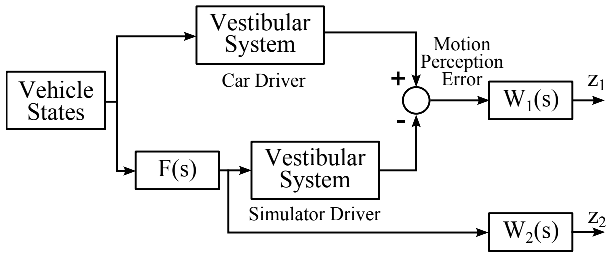

Fig. 3. LQG filter design framework.

$$\underline{L}_j = L_j \underline{\hat{L}}_j = \underline{P}_j - \underline{B}_j \quad (j = 1..6) \tag{4}$$

3. LINEAR OPTIMAL CONTROL

The linear optimal control approach was developed in Sivan et al. [1982], Reid and Nahon [1985], Telban and Cardullo [2005] and was then extended to include frequency-dependent weight as shown in Figure 3. This approach to filter design is based on a model of the human vestibular system with the aim of taking advantage of the body's natural movement filtering processes; the translational accelerations and angular velocities that a person senses are not the same as those that the person actually undergoes.

The translational acceleration and rotational velocity of the actual vehicle form the input to the system. The top signal path represents the driver of the real car, where the motion he/she senses is a filtered version of the real accelerations and angular velocities. The lower signal path represents the simulator. The vehicle accelerations and angular velocities are filtered by $F(s)$ and the resulting motions are rendered by the simulator. The simulator driver's vestibular system filters these signals to yield sensed motions. The motion perception error is the difference between the movement sensed by the simulator and car driver.

This problem can be recast in a generalised regulator form Green and Limebeer [2012] as shown in Figure 4. The vehicle states are modelled as coloured noise processes and the outputs z_1 and z_2 represent the frequency-weighted perception error and platform states (velocities and displacements). LQG theory is then used to design the filter $F(s)$ that minimises the output integral square error. Including the platform states in the cost function results in a trade-off between the perception error and the simulator motion. If the motion is heavily penalised, a larger error will result, and conversely if the error is small an increased motion is required. The frequency weights $W_1(s)$ and $W_2(s)$ are iteratively tuned until, for a sample lap, the platform remains within its workspace constraints. The selection of the weights also affects the shape of the acceleration signal and requires tuning in response to driver feedback.

4. NUMERICAL OPTIMAL CONTROL

The work in this paper makes use of a Guass-Legendre-Radua psuedospectral optimal control solution method that has been implemented in the software package GPOPS-II Patterson and Rao [2013].

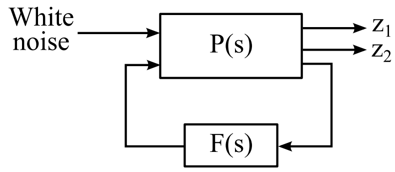

Fig. 4. LQG filter synthesis problem in generalised regulator form.

4.1 Definition of an Optimal Control Problem

The purpose of an optimal control calculation is to determine the state and control associated with a system in order to minimise the performance index Betts [2001]. When expressed in Bolza form, the performance index is given by

$$J = \Phi\left(t_0, x(t_0), t_f, x(t_f), p\right) + \int_{t_0}^{t_f} l(t, x(t), u(t), p)dt, \tag{5}$$

while the system and operating constraints are given by

$$\begin{cases} \dfrac{dx}{dt} - f\left(t, x(t), u(t), p\right) = 0 \\ g\left(t, x(t), u(t), p\right) = 0 \\ h\left(t, x(t), u(t), p\right) \leq 0 \\ g_b\left(x(t_0), x(t_f), u(t_0), u(t_f), p\right) = 0 \end{cases} \tag{6}$$

where $t_0 \leq t \leq t_f$ is the optimisation interval with t_f either fixed, or free to be optimised. The vector $p \in \mathbb{R}^{n_p}$ contains any fixed parameters to be optimised [1] , and $x(t) \in \mathbb{R}^n$ and $u(t) \in \mathbb{R}^m$ are the state and control vectors respectively. The vector-valued function $f(\cdot) \in \mathbb{R}^n$ describes the system dynamics. The vector functions $g(\cdot) \in \mathbb{R}^{n_g}$ and $h(\cdot) \in \mathbb{R}^{n_h}$ define the equality and inequality constraints for the system. The subscript b refers to the boundary constraints with $g_b(\cdot) \in \mathbb{R}^{n_{g_b}}$. The scalar function $l(\cdot)$ is the stage cost that is a function of the state, the controls and the parameters.

Direct methods of the type employed here transcribe, or convert, infinite-dimensional optimal control problems into a finite-dimensional optimisation problem with algebraic constraints; a nonlinear programming problem (NLP).

4.2 Optimal Cueing Problem Formulation

The optimal control problem is formulated as shown in Figure 5. The car acceleration and rotational velocity are the reference signals generated by a minimum lap-time simulation Perantoni and Limebeer [2014]. The optimal control generates a vector control signal $u(t)$ that contains the platform body-fixed accelerations and rotational velocities. Two performance indices are used

$$J_1 = \int_{t_0}^{t_f} e^2 dt \tag{7}$$

$$J_2 = \int_{t_0}^{t_f} (e^2 + \alpha v^2) dt \tag{8}$$

[1] $\mathbb{R}^n$ denotes the set of n-dimensional real vectors.

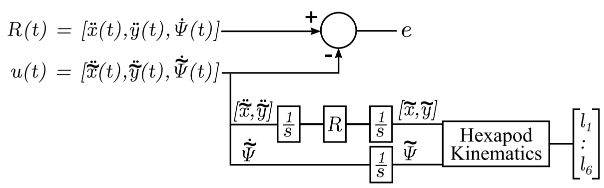

Fig. 5. Open-loop optimal control of the motion platform. The car accelerations are given by $R(t)$, with the washed out platform acceleration signals given by $u(t)$.

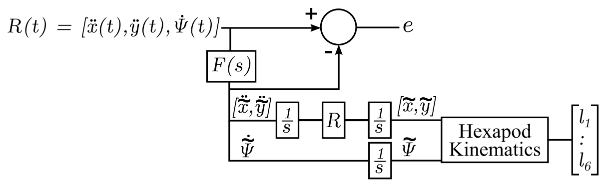

Fig. 6. Alternative formulation of the optimal washout filter synthesis problem. The parameters of the linear filter $F(s)$ are optimised by a nonlinear programming algorithm.

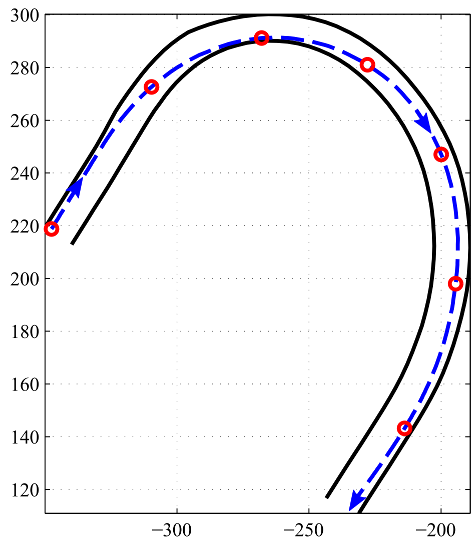

Fig. 7. Turn 4 of the Barcelona Formula One circuit. The optimal racing line is shown as the (blue) oriented dashed line. The (red) time markers are one second apart; the first deemed to be at 0 s and the last at 6 s.

The index (7) seeks to minimise the acceleration error alone, while (8) includes an additional term that penalises the square of the platform's velocity component in the direction of the acceleration demand. As explained in Section 2, the platform's forward kinematics are used to constrain its motion so that it remains within the available workspace.

4.3 Optimal Filter Parameter Design

Numerical optimal control is also used to design linear washout filters. The problem is recast as shown in Figure 6. Instead of the platform accelerations being control inputs they are filtered versions of the reference signals. In this study the filters are fourth order with the filter coefficients free to be optimised. In this form the problem is a parameter optimisation problem, subject to the same kinematic constraints and with the same performance index.

5. RESULTS

5.1 LQG and Optimal Filter Parameter Design

The LQG filters were tuned using simulation data for a complete minimum-time lap of the Circuit de Barcelona-Catalunya so that the resulting hexapod movement remained within the allowed workspace. The same minimum-time lap data was used as the reference in the numerical optimal control problem, which determined the linear filter parameters. The performance of the filters are examined for the long cornering manoeuvre (shown in Figure 7), which features strong braking, acceleration and a period of sustained lateral acceleration.

There are two concepts that need to be defined before analysing the results. The first is onset cues. The idea is to accelerate the platform correctly at the beginning of a manoeuvre and then, when it runs out of workspace, stop the movement for the remainder of the manoeuvre and accept that the driver will only receive visual cues. The second is the notion of miscues, which encompasses a 'multitude of sins'. The most common is the acceleration of the platform in the opposite direction to that of the vehicle simulation, which occurs when the platform needs to slow down as it nears the workspace limits. The magnitude of onset cues and miscues are linked, and this will be explored further with the longitudinal filter for example.

The longitudinal direction contains the largest magnitude accelerations and thus requires a low-gain filter. The filters designed by the two alternative methods are shown in Figure 8. As anticipated, the filters are both high pass, as sustained low-frequency accelerations will cause large displacements and thus associated workspace usage. The cut-off frequency of the filters are both at approximately 2 rad/s, but the low- and high-frequency filter gains differ, with the LQG filter reaching a higher high-frequency gain as well as increasing the attenuation of the lower frequency signals. The results of the filtering of the two cueing approaches are shown in Figure 9. The optimal control approach yields a stronger onset cue, i.e. the initial acceleration is larger, however it then produces a larger miscue. The relationship between the magnitude of the onset and miscue arises from simple physics. If the platform undergoes an acceleration, it will also need to be decelerated in order to remain within the workspace. Hence, the larger the acceleration, the larger the subsequent miscue.

Periods of lateral accelerations tend to be sustained for longer periods than longitudinal braking and acceleration. The lateral cueing filters are shown in Figure 10 with the associated responses given in Figure 11. In the case of lateral accelerations an onset cue is again produced which is then "washed out" with the remainder of the manoeuvre un-cued as a result of workspace restrictions. Once again the parameter-optimised (PO) filter has higher magnitude onset cues, and larger miscues than the LQG filter and the parameter-optimised filter with velocity washout.

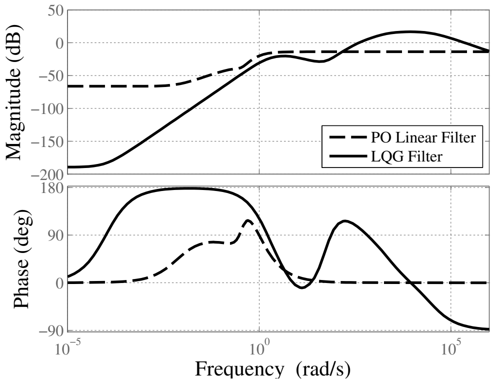

Fig. 8. Longitudinal washout filters designed using the LQG (–) and parameter optimisation methods (PO).

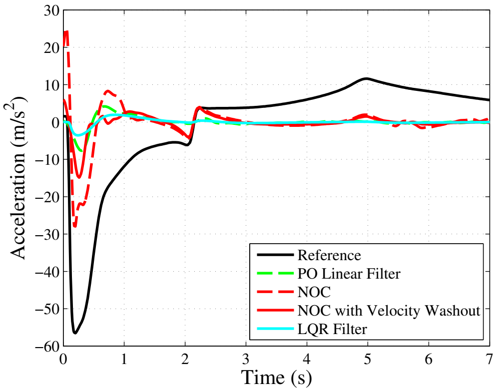

Fig. 9. Comparison of reference and filtered longitudinal accelerations for various cueing strategies.

The yaw filters, also designed using the LQG and PO strategies, can be seen in Figure 12. While both approaches produce high-pass filters, they differ in terms of their numerical detail. As is seen in Figure 13 the two filters have similar onset cues, but the PO filter has a miscue before the manoeuvre, which allows the hexapod to provide a larger angular velocity cue. The LQG filter on the other hand produces a relatively small yaw velocity cue that it then washes out. Both filters preserve the high-frequency information, although this data is not necessarily helpful. Rather than producing a positive angular velocity cue that varies in magnitude, the PO filter produces an oscillatory cue that varies around zero. This is another form of miscue, as it will probably be interpreted by the driver as a change in the vehicle's turning direction.

The biggest drawback of the LQG approach is that it needs to be tuned. Firstly, an estimate of the workspace for each DOF needs to be found, and the filters tuned so that the platform stays within these limits. Then, the filtered signals are combined to calculate the platform actuator lengths. Since the different degrees of freedom are coupled i.e. movement in one freedom reduces the available workspace in another, the filters will need to accommodate this cross coupling. It is never clear which DOF is using the workspace, or which freedom should be reduced. The whole process requires experience, takes time, and does not respect directly the workspace limits.

In contrast, in the numerical optimal control approach the filters are designed so that the platform must respect the

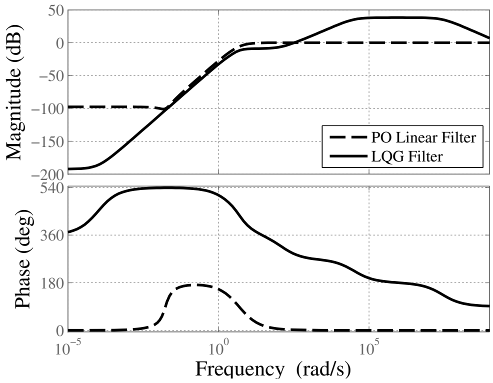

Fig. 10. Lateral washout filters designed with the LQG (–) and PO methods.

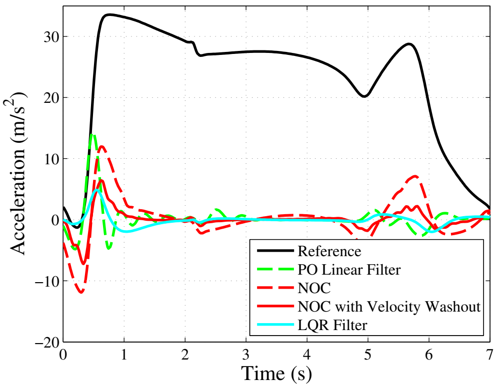

Fig. 11. Comparison of reference and filtered lateral accelerations.

workspace limits. There is one factor that can be adjusted, and this scales the error of the yaw component with respect to the other two error signals. This approach also has the option to limit the individual freedoms in addition to the hexapod constraints. Both approaches produce linear filters, which also have their limitations, and are designed to accommodate worst-case scenarios. Since the negative (braking) accelerations are of a much higher magnitude than the positive ones, the filters are necessarily designed with such low gains that positive accelerations cues tend to be filtered out. This suggests that in future work, the braking and accelerating could be processed with separate filters.

5.2 Open-Loop Optimal Control

The open-loop optimal control problem formulation yields a very different result as compared to those involving linear filters. Structurally, the platform acceleration signals are not restricted to being filtered versions of the vehicle states. Instead, they are open-loop optimal controls in the conventional sense. The selection of the performance index also has a significant impact on the simulators behaviour. Unlike the classical LQG formulation, filter synthesis processes based on numerical optimal control can support hard constraints and non-quadratic cost functions.

The biggest difference between the open-loop optimal control and the linear filters can be seen in the longitudinal acceleration signal (Figure 9). Before a braking manoeuvre the platform is accelerated in the "wrong direction, which

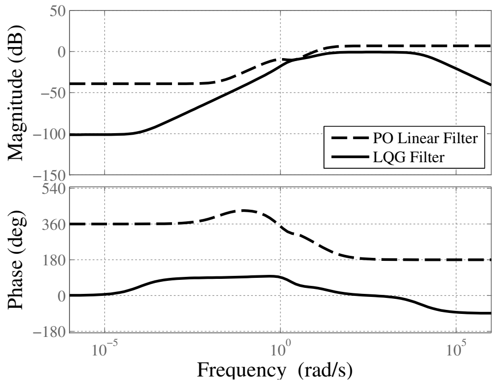

Fig. 12. Yaw washout filters designed using LQG (–) and PO methods.

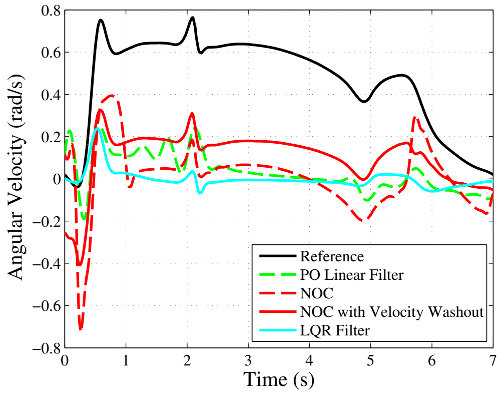

Fig. 13. Comparison of reference and filtered yaw velocities.

allows the system to produce a larger and more sustained acceleration signal; initially to slow the platform down, and then to move it backwards. In addition, there is no washout of the platform to a neutral position, which is common in motion cueing strategies, because the performance index as defined does not call for this type of behaviour. The inclusion of a velocity term in the performance index reduces the magnitude of the false cue that occurs ahead of a manoeuvre, but necessarily also reduces the magnitude of the onset cue. The advantage of this strategy is that the velocity-related term in J_2 provides a method of shaping the cueing signal. Unfortunately open-loop feed-forward cueing cannot be implemented in a practice, because there needs to be some form of feedback response from the driver's. However, these calculations are useful in terms of analysing workspace usage, and examining the feasible accelerations for a given platform.

6. CONCLUSION

We have introduced the use of numerical optimal control techniques into the design of linear filters for race car motion cueing strategies. Numerical optimal control techniques can also be used to assess the capabilities and achievable performance of any simulator motion platform. This approach is able to recognise explicitly the kinematic constraints of the workspace and reduce the need for iterative tuning. An additional benefit comes from the use of real acceleration data rather than coloured noise realisations that are unlikely to be representative of real car behaviour. In the open-loop case, changes to the performance index, such as the introduction of velocity penalties, can be used to alter the characteristics of the resulting cues. The nonlinear programming framework facilitates the extension of the optimal control computations to non-quadratic cost functions. This is a key advantage of this approach and makes it possible to penalise the simulator motion in a nonlinear manner. In this way we hope to take advantage of the nonlinear characteristics of the problem and of human motion perception. This work also has the potential to be developed further to include all six degrees of freedom for use with a 3D car model. The use of optimal-control ideas in a closed-loop system, that does not just use linear filters, also needs to be explored so that the useful characteristics of the open-loop system can be exploited. Finally, the use of non-quadratic performance indices (norms) deserves further attention.

REFERENCES

J.T. Betts. *Practical Methods for Optimal Control Using Nonlinear Programming.* Advances in Design and Control. Society for Industrial and Applied Mathematics, 2001. ISBN 9780898714883.

F. Colombet, M. Dagdalen, G. Reymond, C. Pere, F. Merienne, and A. Kemeny. Motion cueing: What is the impact on the driver's behaviour? In Proceedings of the Driving Simulation Conference DSC Europe, Monaco, France, February 2008.

J. Dichgans and T. Brandt. Visual-vestibular interaction: Effects on self-motion perception and postural control. In *Handbook of Sensory Physiology*, volume 8, pages 755–804. Springer Berlin Heidelberg, 1978.

M. Green and D. J. N. Limebeer. *Linear Robust Control.* Dover, Mineola, New York, 2012.

A.L. Helinski. Dynamic and kinematic study of a Stewart platform using Newton-Euler techniques. Technical report, U.S. Army Tank-Automotive Command, 1990.

C.D. Larsen. Comparison of three degree of freedom and six degree of freedom motion bases utilizing classical washout algorithms. Master's thesis, Iowa State University, 2011.

M. A. Patterson and A. V. Rao. GPOPS-II: A matlab software for solving multiple-phase optimal control problems using hp-adaptive gaussian quadrature collocation methods and sparse nonlinear programming. *ACM Trans. Math. Soft.*, 39:3, July 2013.

G. Perantoni and D.J.N. Limebeer. Minimum-lap-time optimal control for a formula one car with variable parameters. To appear in Vehicle System Dynamics, 2014.

L.D. Reid and M.A. Nahon. Flight simulation motion-base drive algorithm: Part 1 - developing and testing the equations. Technical Report UTIAS Report No. 296, Institute for Aerospace Studies, University of Toronto, Toronto, Canada, 1985.

R. Sivan, J. Ish-Shalom, and J. Huang. An optimal control approach to the design of moving flight simulators. *Systems, Man and Cybernetics, IEEE Transactions on*, Vol:12, Issue:6:818–827, 1982.

R.J. Telban and F.M Cardullo. Motion cueing algorithm development: Human-centred linear and non-linear approaches. Technical report, State University of New York, 2005.